Phenomenological Model for Predicting the Energy Resolution of Neutron-Damaged Coaxial HPGe Detectors

C. DeW. Van Siclen, E. H. Seabury, C. J. Wharton, and A. J. Caffrey

Abstract—**The peak energy resolution of germanium detectors deteriorates with increasing neutron fluence. This is due to hole capture at neutron-created defects in the crystal which prevents the full energy of the gamma-ray from being recorded by the detector. A phenomenological model of coaxial HPGe detectors is developed that relies on a single, dimensionless parameter that is related to the probability for immediate trapping of a mobile hole in the damaged crystal. As this trap parameter is independent of detector dimensions and type, the model is useful for predicting energy resolution as a function of neutron fluence.**

Index Terms—**Germanium detector, energy resolution, neutron damage.**

I. INTRODUCTION

A gamma-ray traversing a germanium crystal loses energy mainly by the production of Compton electrons (or a photoelectron in the case of low-energy gamma-rays), which in turn lose energy by the production of electron-hole pairs at roughly 2.96 eV each. The electrons and holes are collected at the outer and inner electrodes covering the annular surfaces of the cylindrical crystal, thereby recording the energy of the gamma-ray. The full energy is not recovered, however, when holes are trapped at negatively charged defects in the crystal created by a flux of fast neutrons. Thus the energy resolution of gamma-ray peaks deteriorates with fast neutron fluence.

In practice, the gamma-ray energy is determined by measuring the current flow, induced by the *moving* electron and hole charges, between the electrodes. In this phenomenological model, the gamma-ray energy is instead calculated from the integrated charge at the two electrodes, induced by the electron-hole pairs.

This paper is laid out as follows. In section II the relation between an electron-hole pair and the induced charges at the electrodes is derived: this is essentially the concept of the detector. In section III expressions for the spatial density of hole traps (regions of fast neutron damage), and for the interaction cross-section of those traps, are derived. In anticipation of the computer implementation of the model, section IV describes

the stochastic methods for choosing the location of electron-hole pair creation and subsequent location of the hole trapping. In section V the computer program, that combines these pieces of the model to produce spectral line peaks, is described. Finally, model results are compared to measurements, made in our laboratory, of the energy resolution of the 1332 keV ^{60}Co spectral line obtained by a p-type detector irradiated by a fast neutron fluence up to 10^9 cm^{-2}.

The primary purpose of this work is to produce a predictive model of peak energy resolution as a function of fast neutron fluence. It is a phenomenological model, meaning that critical parameters are taken from experiment rather than calculated from first principles. The (dimensionless) critical parameters in this case are α_h, which is related to the hole trap cross-section, and α_t, which is essentially the average number of hole traps created by a fast neutron as it collides with atoms in the germanium crystal. (These are both introduced in section III.) Values for these parameters are obtained by reproducing, with the model, the data of R. H. Pehl *et al.* [1]. In that work, two HPGe coaxial detectors (one n-type, the other p-type), fabricated from the same crystal, were irradiated simultaneously with fast neutrons from an unmoderated ^{252}Cf source.

For the convenience of the reader, SI units (and derived units) are used in any calculations: electric potential ϕ in volts (V); electric field E in V·m^{-1}; force in newtons (n); charge in coulombs (C). Note that 1 V = 1 n·m·C^{-1}. Further, the product $e\,(v\ \text{V}) = v$ eV. The electric charge $e = 1.602 \times 10^{-19}$ C; the vacuum permittivity $\epsilon_0 = 8.854 \times 10^{-12}$ C^2·n^{-1}·m^{-2}.

Where the symbols $\pm$ and $\mp$ occur, the top/bottom sign is used for p-type/n-type detectors. The coaxial detector is an annular cylinder so it is natural to use cylindrical coordinates (r, z): the radius of the inner electrode is R_0; the radius of the outer electrode is R_1; the axial coordinate $z = 0$ at the top of the coaxial detector (the end pointing at the radiation source), and $z > 0$ within the detector.

II. INDUCED CHARGE AT THE ELECTRODES DUE TO ELECTRON-HOLE PAIRS

As an electron and hole have opposite charge, it is not until they move apart under the influence of the driving force $q\mathbf{E}(r)$ that charge is induced at the electrodes. The variable q is the charge of the particle (so equals $+e/-e$ for holes/electrons) and $\mathbf{E}(r)$ is the electric field at the particle location r between the electrodes. In the case of p-type detectors, the outer contact

is positively biased so that the field $\mathbf{E}(r)$ is negative; thus holes move towards the inner contact at R_0 and electrons move towards the outer contact at R_1. In the case of n-type detectors, the inner contact is positively biased so that the field $\mathbf{E}(r)$ is positive; thus holes/electrons move towards the outer/inner contact.

What charges are induced at the electrodes by an electron-hole pair after separation? Expressions for these are easily found by use of Green's reciprocation theorem [2]: For a given arrangement of electrodes, if ϕ is the potential due to a volume-charge distribution ρ and a surface-charge distribution σ, while ϕ' is the potential due to other charge distributions ρ' and σ', then

$$\int_V \rho\phi' d^3x + \int_S \sigma\phi' da = \int_V \rho'\phi d^3x + \int_S \sigma'\phi da. \quad (1)$$

In the "primed" system, set $\rho' = \sigma' = 0$, so $\phi'(r)$ is the solution to Laplace's equation in cylindrical coordinates with boundary conditions $\phi' = 1$ at surface S, which is inner contact R_0, and $\phi' = 0$ at outer contact R_1. Then the right hand side equals zero, so the "unprimed" system (which is the annular cylinder with a point charge at r and a surface charge at the inner contact) obeys the relation

$$\int_V \rho\phi' d^3x = -\int_S \sigma da. \quad (2)$$

Recognizing that ρ (the charged particle at r) is q times the delta function produces the relation $q\phi'(r) = -\int_S \sigma da$. Thus the induced charge at the *inner* contact due to a charged particle at r is

$$Q_0(r) = -q\phi'(r)$$
$$= -q\left(1 - \frac{\ln[r/R_0]}{\ln[R_1/R_0]}\right) = -q\frac{\ln[R_1/r]}{\ln[R_1/R_0]}. \quad (3)$$

Similarly (but setting $\phi' = 1$ at surface S, which is outer contact R_1, and $\phi' = 0$ at inner contact R_0), the induced charge $Q_1(r)$ at the *outer* contact due to a charged particle at r is

$$Q_1(r) = -q\phi'(r) = -q\frac{\ln[r/R_0]}{\ln[R_1/R_0]}. \quad (4)$$

Note that the induced charges $Q_0(r)$ and $Q_1(r)$ at the two electrodes are opposite in sign to the charge q of the particle at r, and that the sum $Q_0(r) + Q_1(r)$ always equals $-q$.

Now consider an electron-hole pair created at r_i. As the two particles are of opposite sign and both reside at r_i, no charge is induced at the two contacts. However, as the two mobile charges separate and move radially to r_e and r_h, respectively, the charge Q_0 is induced at the R_0 contact and the charge Q_1 is induced at the R_1 contact, where

$$Q_0 = Q_0(r_e) + Q_0(r_h) = e\frac{\ln[r_h/r_e]}{\ln[R_1/R_0]} \quad (5)$$

$$Q_1 = Q_1(r_e) + Q_1(r_h) = -e\frac{\ln[r_h/r_e]}{\ln[R_1/R_0]}. \quad (6)$$

It is these induced charges Q_0 and Q_1 that account for the current between the two contacts due to an electron-hole pair (note that an incremental change $\delta Q_0 = -\delta Q_1$ always, as electric charge flows from one contact to the other). Note that initially $r_e = r_h = r_i$ so the induced charges $Q_0 = Q_1 = 0$, and that when both mobile charges successfully reach their respective contacts, the induced charges $Q_0 = \mp e$ and $Q_1 = \pm e$, as expected (top/bottom sign indicates p-type/n-type detector). As the current between electrodes is just the transfer of charge from one to the other, the result $|Q_0| = |Q_1| = e$ allows the full creation energy of the electron-hole pair to be recorded.

For a p-type detector, when the hole is trapped at r_h but the electron successfully reaches R_1, the charge induced at the central contact is $Q_0 = -e\frac{\ln[R_1/r_h]}{\ln[R_1/R_0]}$ and the charge induced at the outer contact is $Q_1 = e\frac{\ln[R_1/r_h]}{\ln[R_1/R_0]}$. Note that in this case $Q_0 = Q_0(r_h)$ and $Q_1 = e + Q_1(r_h) < e$, meaning that $|Q_0| = |Q_1| < e$ so not all of the pair creation energy is recorded. For an n-type detector, when the hole is trapped at r_h but the electron successfully reaches R_0, the induced charges are $Q_0 = e\frac{\ln[r_h/R_0]}{\ln[R_1/R_0]}$ and $Q_1 = -e\frac{\ln[r_h/R_0]}{\ln[R_1/R_0]}$, and again not all of the pair creation energy is recorded. By examining the two expressions for Q_0 (or Q_1), it is evident that in general the average value $\langle|Q_0|\rangle$ for a damaged p-type detector will be less than that for a damaged n-type detector, since a spatially uniform flux of gamma-rays will produce more electron-hole pairs near the outer contact than near the inner contact, so resulting in more hole trapping near the outer contact (thus $\langle\ln[R_1/r_h]\rangle < \langle\ln[r_h/R_0]\rangle$). This effect translates into less energy being attributed to an incident gamma-ray by a p-type detector than by an n-type detector.

The induced charges (currents) at the contacts are related to the energy of the incident gamma-ray in a straightforward way. When the electron and hole reach their terminal locations at r_e and r_h, respectively, the induced charges Q_0 and Q_1 correspond to an energy $\frac{Q}{e}\epsilon$ recorded by the detector, where $Q \equiv |Q_0| = |Q_1|$ and ϵ is the average energy needed to create an electron-hole pair (this is the energy needed to elevate an electron in the valence band into the conduction band). For germanium, $\epsilon = 2.96$ eV at 77 K [3]. An incident gamma-ray of energy E_γ that produces n electron-hole pairs will thus record an energy $n\frac{\langle Q\rangle}{e}\epsilon$, where the average value $\langle Q\rangle$ is taken over all the n pairs.

In the implementation of this model in a computer code, a value for n is chosen for each incident gamma-ray from the Gaussian distribution $p(n) = \left(2\pi\sigma^2\right)^{-1/2}\exp\left[-(n-n_\gamma)^2/(2\sigma^2)\right]$. The average value $n_\gamma = E_\gamma/\epsilon$ [so for example, the 1332 keV ^{60}Co gamma-ray produces (on average) $n_\gamma = 4.5 \times 10^5$ electron-hole pairs in a germanium detector]. The variance $\sigma^2 = F \cdot n_\gamma$ where F is the Fano factor (and is approximately 0.13 for Ge detectors [3]). To obtain values for n from this distribution, it is most convenient to use the Box-Muller method [4]: Consider the "standard normal" distribution $\phi(\nu) = (2\pi)^{-1/2}\exp\left[-\nu^2/2\right]$. Then the two random variables ν_1 and ν_2 will both have the standard normal distribution and will be independent, where

$$\nu_1 = (-2\ln x_1)^{1/2}\cos(2\pi x_2) \quad (7)$$

$$\nu_2 = (-2\ln x_1)^{1/2}\sin(2\pi x_2) \quad (8)$$

and x_1 and x_2 are random numbers taken from the uniform distribution on $(0, 1]$. Then the desired value $n = n_\gamma + \sigma\nu$, where ν is either ν_1 or ν_2 calculated from Eq. (7) or Eq. (8).

Note that the FWHM of the Gaussian distribution $p(n)$ is $2\left(2\sigma^2 \ln 2\right)^{1/2}$. The FWHM of the corresponding energy peak is then $2\left(2Fn_\gamma \ln 2\right)^{1/2} \cdot \epsilon = 2\left(2FE_\gamma \epsilon \ln 2\right)^{1/2}$. So for example, in the absence of neutron damage, the FWHM of the peak corresponding to the 1332 keV ^{60}Co spectral line is 1.686 keV, while that of the peak corresponding to the 122.1 keV ^{57}Co spectral line is 0.510 keV.

III. HOLE TRAPPING

The fate of mobile holes (and electrons) in the neutron-damaged crystal is determined by the spatial distribution of traps, and the trap cross-section. These two functions are derived in turn.

The distribution of particle traps should be uniform over a z-slice (thickness dz), since the source of gamma-rays (at which the detector is pointed) also acts as the primary source of neutrons. What then is the trap density $\rho_q(z)$ (the number of traps in the infinitesimal volume $A \cdot dz$ at axial position z, where A is the cross-sectional area of the crystal)? Consider that the mean free path of an incident neutron is l. That is, the probability that the neutron first collides a distance $[z, z + dz]$ from its entry point into the crystal is $\exp\left[-z/l\right] \cdot (dz/l)$. Then $N \exp\left[-z/l\right] \cdot (dz/l)$ is the number of neutrons that first collide a distance $[z, z + dz]$ from their entry point at $z = 0$, where N is the number of neutrons incident on the crystal. Assuming that the collision produces a trap, the trap density

$$\rho_q(z) = \alpha_t \cdot N \exp\left[-z/l\right] \cdot (dz/l) / (A \cdot dz)$$
$$= \alpha_t \cdot \frac{N}{lA} \exp\left[-z/l\right] \qquad (9)$$

where N/A is the neutron fluence, and the dimensionless parameter α_t is the (average) number of traps created by a fast neutron as it collides with atoms in the germanium crystal. Note that α_t should be somewhat larger than 1, to account—in a crude way—for any subsequent collisions by the neutron.

What is a reasonable value for α_t? For a neutron incident on a detector of length (thickness) L, the probability that *no* collisions occur over the distance L is $\exp\left[-L/l\right]$, meaning that for a neutron fluence N/A, the fraction $1 - \exp\left[-L/l\right]$ undergo at least one collision. L. S. Darken *et al.* [5], after irradiating a 3 cm thick Ge crystal with neutrons, conclude "A fast neutron flux of 10^{10} cm^{-2} produces about 2×10^9 cm^{-3} disordered regions of various sizes". Setting $l = 6$ cm [6] and $L = 3$ cm, the fraction of incident neutrons that underwent collisions in the crystal was 0.3935. Each of those neutrons was then responsible for $\left(2 \times 10^9 \times 3\right) / \left(0.3935 \times 10^{10}\right) = 1.5$ traps per (collided) neutrons. Thus in general $\alpha_t \sim 1.5$.

As charged particles, holes and electrons may be trapped at defects with opposite charge. It is believed that hole traps are large disordered regions with large negative charge [7], and so have a large effective cross-section, while electron traps are much smaller (perhaps point defects) and so have a much smaller cross-section. In any event, the trap cross-section σ_q must be roughly the size of the local distortion, due to the

electric charge of the defect, of the applied electric field $\mathbf{E}(r)$. An expression for σ_q can be derived as follows.

For simplicity, use 2D Cartesian coordinates, and place the defect (with charge Q) at the origin, and set the no-defect electric field $\mathbf{E} = E\hat{\mathbf{x}}$. Then the potential $\phi^*(\mathbf{r})$ at the point $\mathbf{r} = (x, y)$ for this system is $\phi(x) + \frac{Q}{\epsilon}\left(x^2 + y^2\right)^{-1/2}$ where $\phi(x)$ is the potential at $\mathbf{r}$ in the absence of the defect and ϵ is the permittivity of germanium. This produces the electric field

$$\mathbf{E}^*(\mathbf{r}) = -\nabla\phi^*(\mathbf{r}) = \left\{E + \frac{Q}{\epsilon}x\left(x^2 + y^2\right)^{-3/2}\right\}\hat{\mathbf{x}}$$
$$+ \frac{Q}{\epsilon}y\left(x^2 + y^2\right)^{-3/2}\hat{\mathbf{y}}. \qquad (10)$$

The electric field lines in the absence of the defect are directed parallel to the x-axis; in the presence of the charged defect at the origin, they are bent towards the origin. Those field lines that terminate at the defect are particle paths that lead to trapping. Clearly the field lines are seriously bent towards the defect when the magnitude of the y-component $\frac{Q}{\epsilon}y\left(x^2 + y^2\right)^{-3/2}$ of the field $\mathbf{E}^*(\mathbf{r})$ exceeds that of the x-component $E + \frac{Q}{\epsilon}x\left(x^2 + y^2\right)^{-3/2}$; that is, when $x \approx 0$ and $y^2 < \left|\frac{Q}{\epsilon E}\right|$. Thus the trap cross-section $\sigma \sim \pi y^2 \propto \frac{e}{\epsilon E}$. As the electric field $\mathbf{E}(r)$ in the crystal has a radial dependence, $\sigma_q(r) = \alpha_q \cdot \frac{e}{\epsilon}E(r)^{-1}$ where α_q is a dimensionless parameter.

What are reasonable values for α_q? L. S. Darken *et al.* [8] estimate cross-sections $\sigma_h \sim 10^{-11}$ cm^2 and $\sigma_e \sim 10^{-13}$ cm^2. A typical value for $E(r)$ (the magnitude of the electric field in the crystal produced by the bias potential at an electrode) is 125 kV m^{-1}. Thus $\alpha_h \sim 0.1$ and $\alpha_e \sim 10^{-3}$.

Due to the higher production of electron-hole pairs near the outer contact R_1, it is preferable to have a larger electric field E there as well to reduce the trap cross-sections σ_q. This shaping of the electric field is accomplished by doping p-type and n-type germanium detectors with (electron acceptor) boron and (electron donor) lithium, respectively. These dopants produce an intrinsic space (free) charge density $\rho = -e\rho_A$ in the case of p-type detectors and $\rho = e\rho_D$ in the case of n-type detectors [9], where $\rho_{A/D}$ is the density of acceptor/donors. A typical value is $\rho_{A/D} = 10^{10}$ cm^{-3}.

The potential $\phi(r)$ between the contacts satisfies Poisson's equation, $\nabla^2\phi = -\rho/\epsilon$, where $\epsilon = 16\epsilon_0$ is the permittivity of Ge. This equation

$$\frac{1}{r}\frac{d}{dr}\left(r\frac{d}{dr}\phi(r)\right) = -\frac{\rho(r)}{\epsilon} \qquad (11)$$

is solved for $\phi(r)$ given the boundary conditions, which are the applied potentials at the outer and inner contacts. For p-type/n-type detectors, the outer/inner contact is positively biased. The electric field between the contacts is then $\mathbf{E}(r) = -\nabla\phi(r)$.

In the usual case that the charge density ρ has no radial dependence, $\phi(r) = \phi(R_0) - \frac{\rho}{4\epsilon}\left(r^2 - R_0^2\right) + A\ln\left[r/R_0\right]$ and $\mathbf{E}(r) = \left(\frac{\rho}{2\epsilon}r - \frac{A}{r}\right)\hat{\mathbf{r}}$ where the constant

$$A = \frac{\phi(R_1) - \phi(R_0) + \frac{\rho}{4\epsilon}\left(R_1^2 - R_0^2\right)}{\ln\left[R_1/R_0\right]}. \qquad (12)$$

Thus the electric field magnitude $E(r)$, needed to calculate the trap cross-sections $\sigma_q(r)$, is easily obtained.

IV. TRAPPING PROBABILITY

Trapping of a mobile, charged particle (electron or hole) is a stochastic process, meaning that the probability that a particle at r' will be trapped in the infinitesimal distance interval $[r', r' + dr']$ is $\rho_q(z)\sigma_q(r')dr'$. Then the probability that it will *not* be immediately trapped is $1 - \rho_q(z)\sigma_q(r')dr'$, which effectively equals $\exp\left[-\rho_q(z)\sigma_q(r')dr'\right]$. By taking the product of many such exponentials, the probability p_q for the charged particle created at r_i to successfully reach r is

$$p_q\left(r_i, r, z\right) = \exp\left[-\left|\int_{r_i}^{r} \rho_q(z)\sigma_q(r')dr'\right|\right] \qquad (13)$$

where use of the absolute value allows for the case $(r < r_i)$ that the particle moves towards the inner electrode.

The probability for the particle, having been created at the interaction point r_i, to be subsequently trapped in the infinitesimal interval $[r, r + dr]$ is then $-\frac{dp_q(r_i, r, z)}{dr}dr$. To see this, note that

$$-\int_{r_i}^{r} \frac{dp_q\left(r_i, r', z\right)}{dr'}dr' = -p_q\left(r_i, r, z\right) + p_q\left(r_i, r_i, z\right)$$

$$= 1 - p_q\left(r_i, r, z\right) \qquad (14)$$

is the probability that a particle, created at r_i, never arrives at r. Thus the derivative $-\frac{dp_q(r_i, r, z)}{dr} \equiv T_q\left(r_i, r, z\right)$ is the PDF (probability distribution function) for the particle trap position r given r_i.

To perform a computer simulation of particle creation and trapping, a trap position r is randomly selected from this distribution. How is this done? The formula for converting a random number x taken from the *uniform* probability distribution $P(x) = 1$ (such x values are produced by standard random number generators) to the corresponding r value is derived as follows. The probabilities $T_q\left(r_i, r, z\right)dr$ and $P(x)dx$ must be equal, so $T_q\left(r_i, r, z\right)dr = dx$. Then integrating the former from r_i to r, and the latter from 0 to x gives

$$x = \int_{r_i}^{r} T_q\left(r_i, r', z\right)dr'$$

$$= -\int_{r_i}^{r} \frac{dp_q\left(r_i, r', z\right)}{dr'}dr' = 1 - p_q\left(r_i, r, z\right) \qquad (15)$$

which relates a randomly chosen x value to an r value. The function $x(r) = 1 - p_q\left(r_i, r, z\right)$ must be inverted so as to give r when x is chosen randomly from the interval $[0, 1)$; that is, the function $r(x)$ must be found. This is done by expressing the relation as

$$\ln\left[1 - x\right] = \ln\left[p_q\left(r_i, r, z\right)\right] = -\left|\int_{r_i}^{r} \rho_q(z)\sigma_q(r')dr'\right|$$

$$= -\rho_q(z)\frac{\alpha_q e}{16\epsilon_0}\left|\int_{r_i}^{r} \frac{dr'}{E(r')}\right|. \qquad (16)$$

This integral can be solved analytically by noting that $E(r)^{-1} = \frac{r}{-A + \frac{\rho}{2\epsilon}r^2}$, giving (after some careful algebra)

$$\ln\left[1 - x\right] = \pm\frac{q}{e}\rho_q(z)\frac{\alpha_q}{\rho_{\text{A/D}}}\ln\left[\frac{-A + \frac{\rho}{2\epsilon}r^2}{-A + \frac{\rho}{2\epsilon}r_i^2}\right] \qquad (17)$$

under the condition that $\rho \neq 0$ (i.e., that the crystal is doped).

If the x value chosen from the interval $[0, 1)$ is greater than $1 - p_q\left(r_i, R, z\right)$, where R is the radius of the contact to which the particle is moving, then the particle has successfully reached that contact. That is, if the x value satisfies the relation

$$\ln\left[1 - x\right] \leq \pm\frac{q}{e}\rho_q(z)\frac{\alpha_q}{\rho_{\text{A/D}}}\ln\left[\frac{-A + \frac{\rho}{2\epsilon}R^2}{-A + \frac{\rho}{2\epsilon}r_i^2}\right] \qquad (18)$$

then the particle has successfully reached the contact at radius R. Otherwise the position r at which the particle is trapped is obtained from the equation

$$r^2 = \frac{2\epsilon}{\rho}\left\{A + \left(-A + \frac{\rho}{2\epsilon}r_i^2\right)(1 - x)^{\pm\frac{q}{e}\frac{\rho_{\text{A/D}}}{\rho_q(z)\alpha_q}}\right\}. \qquad (19)$$

A similar stochastic approach is taken for obtaining r_i, the radial location at which a gamma-ray enters the crystal. For simplicity, the gamma-ray is assumed to shed n electron-hole pairs at random points (r_i, z) as it traverses the length of the crystal. Since the z-axis of the detector points at the gamma-ray source, the areal distribution of r_i in a simulation should be uniform over a z-slice of the crystal. Thus the areal density of r_i points is constant: call it ρ_i (points per area). Then $dx = \rho_i dA$ giving

$$x = \frac{\int_{R_0}^{r_i} \rho_i dA}{\int_{R_0}^{R_1} \rho_i dA} = \frac{\int_{R_0}^{r_i} \rho_i 2\pi r dr}{\int_{R_0}^{R_1} \rho_i 2\pi r dr} = \frac{r_i^2 - R_0^2}{R_1^2 - R_0^2}. \qquad (20)$$

Inverting the function $x\left(r_i\right)$ gives

$$r_i = \left\{R_0^2 + x\left(R_1^2 - R_0^2\right)\right\}^{1/2} \qquad (21)$$

from which a value r_i is obtained by randomly choosing a value x from the interval $[0, 1]$.

V. SIMULATION ALGORITHM

The pieces developed above are assembled into a computer model of a coaxial HPGe detector. The inputs are the parameter values for the detector $(R_0, R_1, L, \phi\left(R_0\right), \phi\left(R_1\right), \rho_{\text{A/D}})$, the spectral line (E_γ) of interest, and the neutron fluence N/A. Then the model considers the gamma-rays emitted from a source to be normally incident on the $z = 0$ (top) surface of the detector; subsequently each gamma-ray maintains its radial position r_i and produces n electron-hole pairs as it traverses the length of the crystal. For each gamma-ray, the values r_i and n are obtained stochastically according to Eq. (21) and as described at the end of section II, respectively, and the n pair creation points (r_i, z) are distributed randomly over the length L (that is, the z value for a pair is taken randomly from the interval $[0, L]$ of the uniform distribution).

The contribution of each electron-hole pair to the recorded energy of the gamma-ray is obtained by the following steps: (i) The trap density $\rho_q(z)$ is calculated for each particle by Eq. (9). (ii) This allows the terminal positions r_e and r_h to be obtained stochastically according to Eqs. (18) and (19).
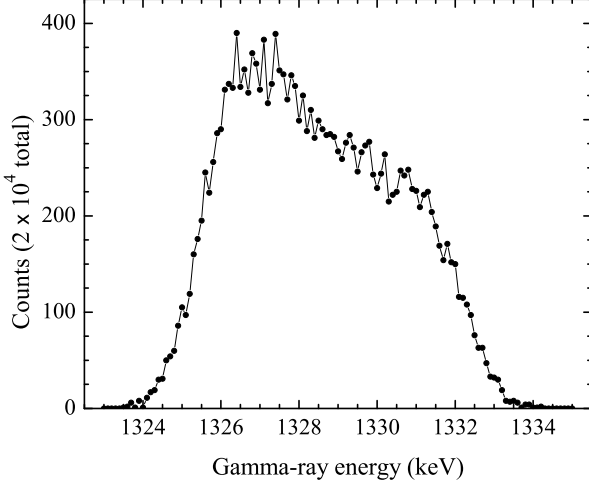
Fig. 1. Peak corresponding to the 1332 keV ^{60}Co spectral line obtained by the p-type detector model for a neutron fluence of 10^9 cm^{-2}. This model detector has the same dimensions and bias potential as the p-type detector studied by Pehl *et al.* [1].

Fig. 2. Peak corresponding to the 1332 keV ^{60}Co spectral line obtained by the p-type detector model for a neutron fluence of 10^{10} cm^{-2}. This model detector has the same dimensions and bias potential as the p-type detector studied by Pehl *et al.* [1].

(iii) Using these values r_e and r_h, the induced charge Q_0 at the inner electrode is calculated by Eq. (5). (iv) Then the contribution of the electron-hole pair to the recorded energy is $(|Q_0|/e) \times 2.96$ eV. The contributions of all n pairs constitute the recorded energy of the gamma-ray.

The energy peak is constructed as a histogram of the gamma-ray energies. The finite width of the peak is due to the variation in the n value (around the average value n_γ) for gamma-rays producing the peak, and to hole and electron trapping suffered by some fraction of the n pairs produced by each gamma-ray. Thus the width of the peak can be modified by adjusting the values of the dimensionless parameters α_t and α_q, or rather, the *product* $\alpha_t \cdot \alpha_q \equiv A_q$. According to section III, the value A_h should lie in the range $[0.1, 1]$, and A_e should be two orders of magnitude or so smaller.

This "tuning" is accomplished by reproducing the data of R. H. Pehl *et al.* [1]. As mentioned above, two HPGe coaxial detectors (one n-type, the other p-type), fabricated from the same crystal, were irradiated simultaneously with fast neutrons from an unmoderated ^{252}Cf source. The input to the model is the following: inner radius $R_0 = 4$ mm; outer radius $R_1 = 21$ mm; crystal length $L = 30$ mm; bias potential for the p-type detector $\phi(R_1) = 1.6$ kV; bias potential for the n-type detector $\phi(R_0) = 2.8$ kV. As dopant densities are not provided, the typical value $\rho_{A/D} = 10^{10}$ cm^{-3} is used. The key data point from Ref. [1] is the FWHM resolution of 6 keV for the 1332 keV ^{60}Co line obtained by the p-type detector after a neutron fluence of 10^9 cm^{-2}. This experimental result is reproduced by the model when $A_h = 0.30$ (and $A_e = 0.001$), as shown in Fig. 1.

As a check (since in fact the energy resolution is very sensitive to the value of A_h), the model gives the FWHM resolution of 64 keV after a neutron fluence of 10^{10} cm^{-2} (as shown in Fig. 2), to be compared with the experimental result of 70 keV. Figures 3 and 4 show the corresponding model results for the n-type detector (model/experimental FWHM
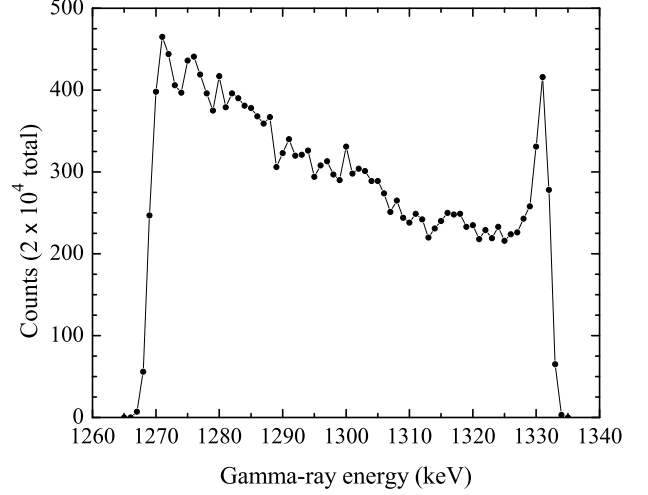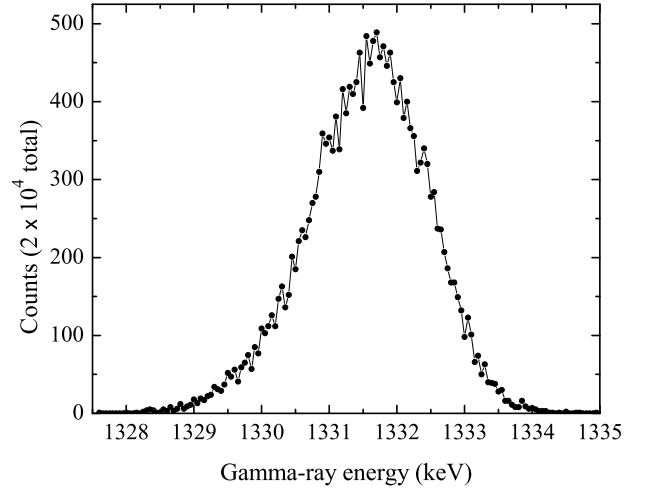

Fig. 3. Peak corresponding to the 1332 keV ^{60}Co spectral line obtained by the n-type detector model for a neutron fluence of 10^9 cm^{-2}. This model detector has the same dimensions and bias potential as the n-type detector studied by Pehl *et al.* [1].

resolutions of $2.1/1.95$ keV and $2.7/2.7$ keV, respectively).

Figures 5 and 6 show the model results for the p-type and n-type detectors, respectively, after a neutron fluence of 10^8 cm^{-2} (model/experimental FWHM resolutions of $1.85/2.1$ keV and $1.80/1.8$ keV, respectively). For this low fluence the model FWHM resolutions are nearly identical for the two detectors; instead the effect of hole trapping shows up in the magnitude of the shift of the peak centroid away from 1332 keV.

VI. Application to the INL Micro-Detective

We exposed an ORTEC Micro-Detective (p-type) detector to a neutron fluence (from a ^{252}Cf source) up to 10^9 cm^{-2}. This exercise was intended to determine the neutron fluence
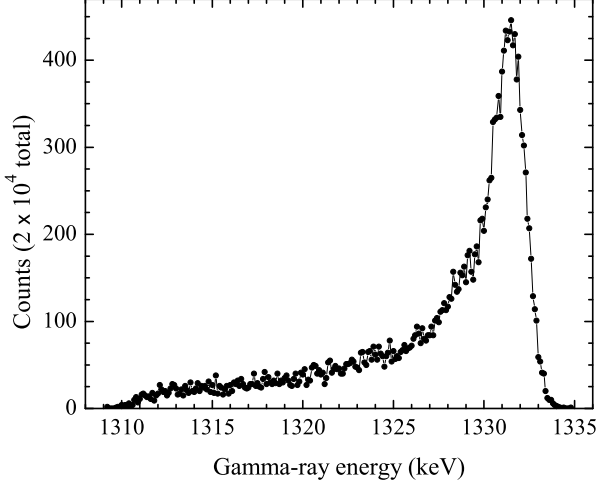
Fig. 4. Peak corresponding to the 1332 keV ^{60}Co spectral line obtained by the n-type detector model for a neutron fluence of 10^{10} cm^{-2}. This model detector has the same dimensions and bias potential as the n-type detector studied by Pehl *et al.* [1].
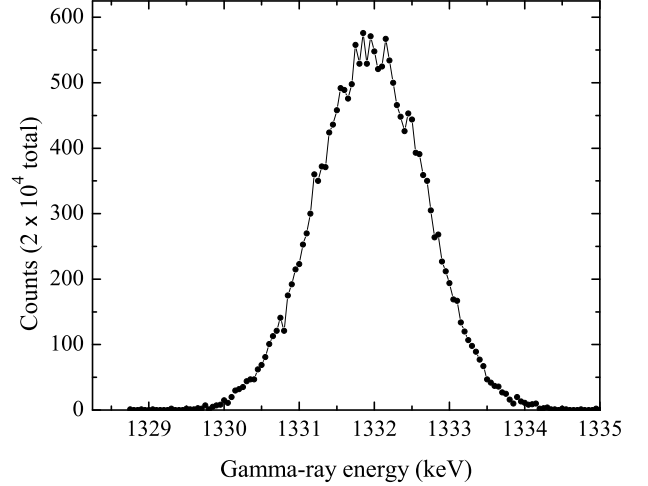

Fig. 6. Peak corresponding to the 1332 keV ^{60}Co spectral line obtained by the n-type detector model for a neutron fluence of 10^{8} cm^{-2}. This model detector has the same dimensions and bias potential as the n-type detector studied by Pehl *et al.* [1].
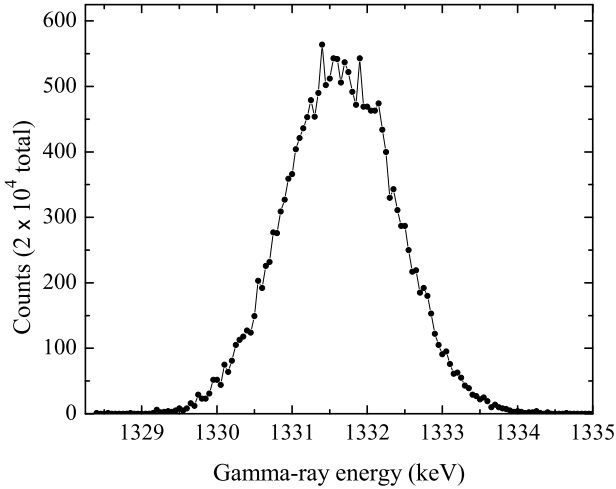

Fig. 5. Peak corresponding to the 1332 keV ^{60}Co spectral line obtained by the p-type detector model for a neutron fluence of 10^{8} cm^{-2}. This model detector has the same dimensions and bias potential as the p-type detector studied by Pehl *et al.* [1].
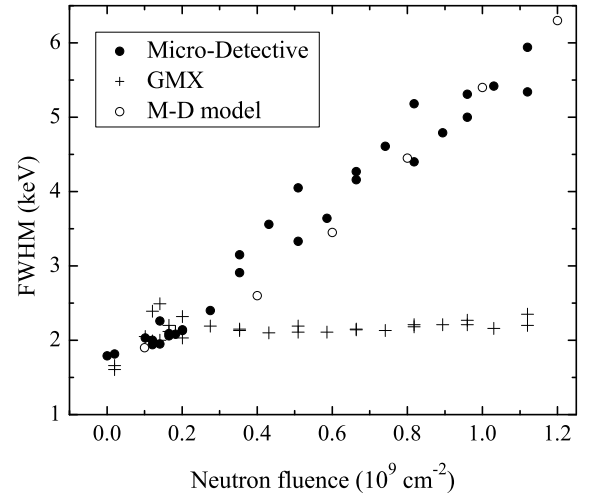

Fig. 7. Measured FWHM resolution of the 1332 keV ^{60}Co peak obtained by the Micro-Detective and GMX detectors after various neutron fluences (where two values are shown for the same fluence, the higher/lower value was measured before/after a thermal cycle). The calculated values obtained by the Micro-Detective model are indicated by the open circles.

at which the energy resolution of the Micro-Detective was too degraded to allow its use in place of our GMX (n-type) detector. Figure 7 shows values of the FWHM resolution of the 1332 keV ^{60}Co peak obtained by the Micro-Detective and GMX detectors at various fluences (where two values are provided for the same fluence, the higher/lower value was measured before/after a thermal cycle). These results provide an opportunity to test the phenomenological model.

The input to the Micro-Detective model is the following: inner radius $R_0 = 4.5$ mm; outer radius $R_1 = 25$ mm; crystal length $L = 30$ mm; bias potential $\phi(R_1) = 3.0$ kV. As the dopant density is not provided, the typical value $\rho_A = 10^{10}$ cm^{-3} is used. The calculated values of the FWHM resolution, indicated by the open circles in Fig. 7, compare well with

the trend of measured values. Note that the energy resolution of the Micro-Detective after a neutron fluence of 10^{9} cm^{-2} is better than that of the p-type detector studied by Pehl *et al.* (5.4 keV versus 6 keV) despite its significantly larger size (diameter 50 mm versus 42 mm), due to its larger bias potential (3 kV versus 1.6 kV) which, by producing a stronger electric field across the crystal, reduces the hole trap cross-section.

The input to the GMX (n-type) detector model is the following: inner radius $R_0 = 5.6$ mm; outer radius $R_1 = 31.4$ mm; crystal length $L = 70.3$ mm; bias potential $\phi(R_0) = 5.0$ kV. As the dopant density is not provided, the typical value $\rho_D = 10^{10}$ cm^{-3} is used. The calculated FWHM resolutions of the 1332 keV peak at neutron fluences of 10^{8} cm^{-2} and 10^{9}

cm^{-2} are 1.7 keV and 2.0 keV, respectively, in good agreement with the measured values in Fig. 7.

VII. CONCLUDING REMARKS

The main attributes of this model of neutron-damaged coaxial HPGe detectors are (i) the use of induced charge at the electrodes to determine the contribution of an electron-hole pair to the measured gamma-ray energy, and (ii) the use of stochastic methods to simulate what are, in fact, stochastic processes. The data of R. H. Pehl *et al.* [1] provided a value for the dimensionless parameter A_h, related to the probability for immediate trapping of a mobile hole, needed to complete the phenomenological model. As the model is, for the most part, one-dimensional, it is easy to implement in a computer code. However, by ignoring the detector "cap" (where the applied electric field is not purely radial), this model is not well suited for application to low-energy gamma-rays which may be substantially stopped in that volume.

Some observations: (i) The n-type detectors maintain good energy resolution to neutron fluences of at least 10^9 cm^{-2}. The noticeable effect of neutron damage is to shift the peak centroid to a lower energy. (ii) The peak shapes after a high neutron fluence of 10^{10} cm^{-2} are very different for p-type and n-type detectors. This is due not only to more hole trapping in a p-type detector, but also to the fact that an electron-hole pair with a trapped hole near the outer contact induces a smaller charge $|Q|$ at the two electrodes of a p-type detector than at the electrodes of a same-sized n-type detector (see section II for a more precise discussion of this effect). Thus those gamma-rays that interact closer to the outer contact (which is to say, most of the gamma-rays) are more likely to register as "counts" at the low/high end of the energy spectrum in the case of p-type/n-type coaxial detectors.

REFERENCES

[1] R. H. Pehl, N. W. Madden, J. H. Elliott, T. W. Raudorf, R. C. Trammell, and L. S. Darken, Jr., "Radiation damage resistance of reverse electrode Ge coaxial detectors," *IEEE Trans. Nucl. Sci.*, vol. NS-26, no. 1, pp. 321–323, Feb. 1979.

[2] J. D. Jackson, *Classical Electrodynamics*. New York: Wiley, 1962.

[3] G. F. Knoll, *Radiation Detection and Measurement*, 3rd ed. New York: Wiley, 2000.

[4] G. E. P. Box and M. E. Muller, "A note on the generation of random normal deviates," *Ann. Math. Statist.*, vol. 29, no. 2, pp. 610–611, 1958.

[5] L. S. Darken, Jr., R. C. Trammell, T. W. Raudorf, R. H. Pehl, and J. H. Elliott, "Mechanism for fast neutron damage of Ge(HP) detectors," *Nucl. Instrum. Methods*, vol. 171, pp. 49–59, 1980.

[6] T. W. Raudorf and R. H. Pehl, "Effect of charge carrier trapping on germanium coaxial detector line shapes," *Nucl. Instrum. Methods Phys. Res. A*, vol. A255, pp. 538–551, 1987.

[7] L. S. Darken, "Role of disordered regions in fast-neutron damage of HPGe detectors," *Nucl. Instrum. Methods Phys. Res.*, vol. B74, pp. 523–526, 1993.

[8] L. S. Darken, Jr., R. C. Trammell, T. W. Raudorf, and R. H. Pehl, "Neutron damage in Ge(HP) coaxial detectors," *IEEE Trans. Nucl. Sci.*, vol. NS-28, no. 1, pp. 572–578, 1981.

[9] Th. Kröll and D. Bazzacco, "Simulation and analysis of pulse shapes from highly segmented HPGe detectors for the γ-ray tracking array MARS," *Nucl. Instrum. Methods Phys. Res. A*, vol. 463, pp. 227–249, 2001.